Hierarchical coupled driving-and-charging model of electric vehicles, stations and grid operators

Benoit Sohet, Yezekael Hayel, Olivier Beaude and Alban Jeandin

Abstract—**The decisions of operators from both the transportation and the electrical systems are coupled due to Electric Vehicles' (EVs) actions. Thus, decision-making requires a model of several interdependent operators and of EVs' both driving and charging behaviors. Such a model is suggested for the electrical system in the context of commuting, which has a typical trilevel structure. At the lower level of the model, a congestion game between different types of vehicles gives which driving paths and charging stations (or hubs) commuters choose, depending on travel duration and energy consumption costs. At the middle level, a Charging Service Operator sets the charging prices at the hubs to maximize the difference between EV charging revenues and electricity supplying costs. These costs directly depend on the supplying contract chosen by the Electrical Network Operator at the upper level of the model, whose goal is to reduce grid costs. This trilevel optimization problem is solved using an optimistic iterative algorithm and simulated annealing. The sensitivity of this trilevel model to exogenous parameters such as the EV penetration and an incentive from a transportation operator is illustrated on realistic urban networks. This model is compared to a standard bilevel model in the literature (only one operator).**

Index Terms—**Electric vehicles, Trilevel optimization, Smart charging, Coupled transportation-electrical systems**

I. INTRODUCTION

Electric Vehicles (EVs) are a promising solution to reduce greenhouse gas emissions and local pollution (air quality, noise). Considering policies and targets around the world, EVs should account for 7 % of the global vehicle fleet by 2030 [1]. This represents an opportunity for the different stakeholders of electric mobility, but also challenges for the grid: in France for example, standard predictions give a 2.2 to 3.6 GW power demand increase during winter peak periods in 2035 [2]. Challenges already arise nowadays due to significant local penetrations of EVs[1], which may lead to local grid constraints and infrastructure investment costs. Therefore, decision-making models are needed to help electric mobility operators with their infrastructure investments and pricing mechanisms, which exploit EV flexibility, in particular during charging.

B. Sohet and Y. Hayel are with LIA/CERI, Univ. of Avignon, 84911, Avignon, FRANCE (e-mail: yezekael.hayel@univ-avignon.fr).

B. Sohet, O. Beaude are with EDF R&D, OSIRIS Dept, EDF Lab' Paris-Saclay, 91120, Palaiseau, FRANCE (e-mail: {benoit.sohet, olivier.beaude}@edf.fr).

A. Jeandin is with Izivia, EDF group, 92419, Courbevoie, FRANCE (e-mail: alban.jeandin@izivia.com).

[1]More than 80,000 EVs in circulation in Paris region: https://www.statistiques.developpement-durable.gouv.fr/sites/default/files/2020-04/immatriculations_neuves_2019.zip

Note that key components of the charging operation of EVs depend on their driving strategies, like the charging place and hours. The driving and charging decisions of EV users (here referred to as "EVs") are thus interdependent, which couples the electrical and the transportation systems, especially in urban networks. This coupling is easily conceivable when during widespread holidays departures most of driving EVs need to charge at public charging stations, where there could be significant waiting time and reduction of available power. Therefore, due to EVs, infrastructure and pricing strategies of an operator of the transportation or the electrical system not only have an impact on the other operators of the same system, but also on the operators of the other system. For example, Park & Ride hubs installed at a city's outskirt by local authorities to mitigate traffic congestion and pollution[2] are also an opportunity for "smart charging".

Models of this coupled electricity-transportation system are suggested in works identified in the review paper [3] and in more recent papers. In [4] and [5], some operator controls an EV fleet and solves the vehicle routing problem to minimize both EVs costs (travel and charging duration and cost) and grid costs. Some papers focus instead on independent EV drivers who learn the optimal driving path and charging station to stop, like in [6] or in one of our previous works [7]. Review paper [3] distinguishes between expansion planning of charging stations as in paper [8], and coordinated operation of a fixed coupled electricity-transportation system, such as the present paper. Among coordinated operation papers whose goal is to design price incentives, some are based on a real-time model of EVs like [9]. This often entails simplifications such as electrical grid constraints neglected in [10], or a coarse zone model of the transportation network in [11].

The present paper adopts a stationary EV model point of view in order to better focus on operators' long-term incentives, like the ones presented in the coordinated operation papers [12], [13] mentioned in review [3], and in more recent papers [14], [15]. At the lower level, EVs behavior is modeled as the equilibrium of a driving-and-charging game: EVs choose the resources (driving path, charging station...) with minimal costs – either financial (traffic tolls, charging cost) or temporal (travel duration, queuing and charging times) – which are function of the other EVs' strategies, due to congestion effects. At the upper level, an urban planner from the transportation and/or the electrical system incites these EVs through pricing mechanisms to adopt "optimal" behavior.

[2]20,000 parking spaces at Paris gates: https://data.iledefrance-mobilites.fr/explore/dataset/parcs-relais-idf/

However, the reduction in the literature of the electrical system's management to one type of operator is particularly unrealistic. Concerning electric mobility, the electrical operators carry out two main functions: the Charging Service to EVs (guaranteed by Operators called CSOs) and the management of the Electrical Network (done by the ENO). In this work, a CSO brings together both the charge point operator in charge of the station and the mobility service provider which deals with the EV customers, and the ENO is both the grid manager and the electricity provider. In the previously mentioned papers, smart charging pricing is chosen to optimize either the ENO's [14] or the CSOs payoff [9], but the interaction between CSO and ENO is not considered. In this work, we use instead a trilevel setting, with the EVs at the lower level, the CSOs at the middle one and the ENO at the upper level. In a future work, we will consider the interaction between several CSOs on top of EVs' game, as in papers [9] and [16]. Other works such as [17], [18] also consider several CSOs, but in a futuristic electricity market environment rather than the current realistic framework of CSOs buying electricity from suppliers (the ENO in the present paper).

In electrical systems, trilevel frameworks are commonly employed in cyber security [19], expansion planning [20] or demand-side management [21], but to our knowledge, only two papers on electric mobility use a trilevel setting. In [22], the ENO chooses the wholesale electricity prices for each charging station. Each station charges its EVs, which only choose the charging quantity depending on the local retail electricity price set by the CSO of the corresponding station. Due to the simple formulations of the three levels objective functions (no game between EVs), this trilevel setting is easily solved analytically. In [23], EVs choose a driving path, a station and a charging quantity. The CSOs choose the local retail prices in order to minimize their costs (the electricity bought from the ENO) and the time EVs spend on the road. The ENO chooses the local wholesale prices for each station to minimize its costs (related to electrical grid constraints) and the time EVs spend on the road. Note that the lower level is not a game but simply an optimization problem as there is no interaction between EVs. The trilevel optimization is solved iteratively: the ENO updates the wholesale prices, then the CSO uses an analytical expression to compute the optimal retail prices. The theoretical and algorithmic details are not specified in this work.

The contributions of this paper can be summarized as follows. First note that, although they were two original contributions of our previous paper [24], this work still relies on two features which are unique in the coupled electrical-transportation literature:

- considering commuting and EVs charging during a whole working day gives the possibility for smart charging mechanisms on top of pricing incentives;
- a charging price at a given hub which depends on the smart charging load at this hub. This price is a congestion cost function which can be nonseparable (i.e., not only depends on congestion nearby, but on all over the

TABLE I: Table of main notations

Abbreviations	
CSO	Charging Service Operator
ENO	Electrical Network Operator
EV / GV	Electric / Gasoline Vehicles
Hub	Park & Ride charging station
LMP	Locational Marginal Price
P&C	Plug and Charge
PT	Public Transport
SC	Smart Charging
WE	Wardrop Equilibrium
Parameters	
i_r	Parking (and charging) hub associated to path r
r_S	Path r + charging at hub
r_H	Path r + charging later (e.g., at home)
$\mathcal{H}_{\text{cso}}$	Set of CSO's hubs
e_1	EV class that can charge at hub or later
e_0	EV class that can only charge at hub
X_e	EV penetration
t_i	PT fare from hub i to destination
λ_i	Charging unit price (9) at CSO's hub $i \in \mathcal{H}_{\text{cso}}$
λ_S^0	Constant charging unit price at city's hub $i \in \mathcal{H} \backslash \mathcal{H}_{\text{cso}}$
λ_H^0	Constant charging unit price at home
L_i	Charging need aggregated over all EVs charging at hub i
Π_{mid}	CSO's objective (charging revenues − supply contract)
Π_{up}	ENOS's objective (supply contract − grid costs)
Variables	
$x_{s,r}$	Flow rate of vehicle class s on path r
$x_{s,a}$	Flow rate of vehicle class s on arc a ($= \sum_{\{r \text{ s.t. } a \in r\}} x_{s,r}$)
$\ell_{i,t}$	Aggregated charging power at hub i and time slot t
α	Charging unit price magnitude (CSO's decision variable)
P	Elec. supplying contract threshold (ENO's decision variable)

network) thus requiring new theoretical results to study the uniqueness of the equilibrium of EVs' game.

The original contributions of the present paper are:

1) a realistic model of commuting and charging at work using a trilevel setting, intended for and solved by the ENO, at the upper level. The CSO and ENO maximize their payoffs using realistic pricing mechanisms and EVs interact both while driving and charging in a coupled game;
2) a new theoretical proof of the unique aggregated charging need at each hub at the equilibrium of the coupled routing-and-charging game between EVs.
3) a carefully designed iterative algorithm solving the trilevel model using simulated annealing, Brent's method and convex optimization, with a theoretical proof of the global algorithm's convergence;
4) sensitivity results on a realistic setting and a comparative study of our trilevel model with a bilevel setting (ENO and CSO combined together in a unique operator using Locational Marginal Pricing), standard in the literature [12], [13].

The paper is organized as follows. The objectives and available strategies of the three types of agents considered (EVs, CSO and ENO) are introduced in Sec. II. The theoretical trilevel model of the interactions between these agents is given in Sec. III. An algorithmic solution of this trilevel optimization problem is studied in Sec. IV and applied in Sec. V to examine the sensitivity of our model to exogenous parameters and compare it to the standard model in literature. Finally, conclusions and perspectives are given in last section.

II. A SMART COUPLED DRIVING-AND-CHARGING MODEL WITH THREE TYPES OF ACTORS

The smart charging use case considered in this work is about commuting: drivers, coming from different places, choose their path to get to their workplace, which are all located in a same city or urban area. In this city, there are Park & Ride hubs where EV users may leave their car charging during working hours, and finish the commuting to their workplace by foot or public transport. In addition to drivers, there are two other types of agents/operators considered in this system:

- The CSOs which are in charge of several hubs and decide the corresponding smart charging fares;
- The ENO which is in charge of the grid of the city considered (assumed to be a medium-voltage one) and which specifies the electricity supply contract with CSOs.

Note that the operators do not control vehicles (in the sense of Vehicle Routing Problems) but only send incentives to influence both the driving and charging decisions of drivers (who interact through congestion effects in the sense of routing games).

A. Vehicle users: a coupled driving-and-charging decision

The transportation network is modeled by a graph in which each arc represents a street (illustrated in Fig. 1). Here a path r refers to the successive arcs used to go from an origin O to the hub i_r chosen to park the vehicle, and also includes the public transport arc connecting i_r to the workplace destination D. Vehicle users have to choose one of the path to go from their origin to their destination, depending on the commuting duration and on the energy consumption costs.

Vehicles are of two distinct types: EVs (index e) and Gasoline Vehicles (GVs, index g) which rely on thermal engines. EVs are split into two classes: EVs in class e_1, when choosing a path r, can either decide to charge at hub i_r during working hours (fictitious path denoted r_S), or only park there and charge later, e.g. at home (path r_H). EVs in class e_0 do not have enough energy (their State of Charge, or SoC, is low) to go home after work and will automatically choose to charge at the hub (path r_S). Vehicles of a same class (g, e_0 or e_1) share the same costs, but more vehicle classes could be considered in order to distinguish for example pure EVs from plug-in hybrid vehicles.

The duration cost of a path r is the same for all vehicle classes and is made of two parts. The first one reflects congestion on each road a composing path r following the Bureau of Public Road (BPR) function [25]:

$$d_a(x_a) = \tau \frac{l_a}{v_a}\left(1 + 2\left(\frac{x_a}{C_a}\right)^4\right),\qquad(1)$$

with $x_a = x_{g,a} + x_{e_0,a} + x_{e_1,a}$ the total flow of vehicles of all classes on arc a, l_a its length, v_a the corresponding speed limit and C_a its capacity. The internal parameters of the BPR function are determined in accordance with [26] for urban area congestion measures. The value of time τ transforms the travel duration into a monetary cost. Note that this congestion cost depends on the drivers path choice through variable x_a. The
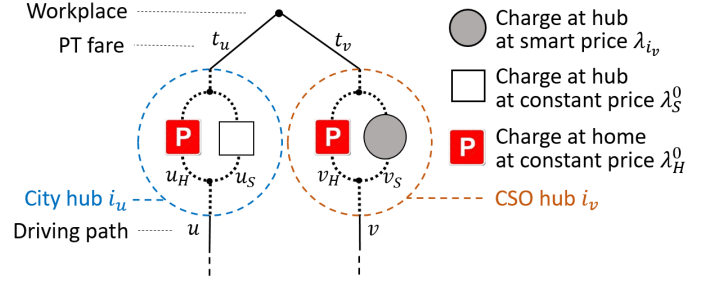

Fig. 1: Illustration of a transportation network. *Each path $r \in \{u, v\}$ includes the driving path to get to the hub i_r associated to r and the PT fare t_r to go from hub i_r to the workplace. At hub i_r, it is possible to only park there and charge later at constant price λ_H^0 (the corresponding global path is written r_H); or, it is possible to charge at the hub (r_S). Considering the latter decision, the charging price at hub i_r is constant (λ_S^0) if the hub is managed by the City authority (like hub i_u). Otherwise, if the hub is managed by the CSO (like hub i_v) then the charging price λ_{i_v} is smartly designed by the CSO.*

second part of the duration cost is a constant t_i representing, if any, the time (expressed as a cost) to go from the hub i where a vehicle is parked to its workplace. Note that other constant costs can be added to t_i like public transport fares.

The second type of cost for drivers is related to energy consumption. The charging fare at hub i is more precisely a charging unit price λ_i, i.e. per unit of energy used, and is specified in the next section. EVs deciding to charge during working hours will be charged up to full SoC. More precisely, the amount of energy EVs of class e_j charge at the hub is equal to the energy consumed while driving to their workplace, plus the difference s_j between full SoC and the SoC before the morning trip. The former quantity of energy is assumed to depend only on the travelled distance, i.e. the energy m_s consumed by a vehicle of class s per distance unit is constant. Thus, EVs of class e_j charging at the hub i_r of path r have to pay:

$$\ell_{e_j,r} \times \lambda_{i_r}, \quad \text{with} \quad \ell_{e_j,r} = (l_r m_e + s_j),\qquad(2)$$

where l_r is the total length of path r. Then, the energy consumed by an EV on path r is approximated by the product $l_r m_e$. A more realistic consumption model – which also depends on the driving speed and exogenous weather conditions (for auxiliary consumption) – would be an interesting follow-up of this work. It is assumed that EVs which do not charge at the hubs also take into account a consumption cost: $\ell_{e_j,r}\lambda_H^0$, with λ_H^0 a constant corresponding to the charging unit price at home for example. Similarly, the consumption cost for GVs is $\ell_{g,r}\lambda_g$ with $\ell_{g,r} = l_r m_g$. The total cost for a vehicle of class s choosing path r is:

$$c_{s,r}(\boldsymbol{x}) = \sum_{a \in r} d_a(x_a) + t_{i_r} + \ell_{s,r}\lambda,\qquad(3)$$

where λ is equal to λ_g if $s = g$, λ_H^0 if $s = e_1$ and $r = r_H$ or λ_{i_r} if $s = e_j$ and $r = r_S$.

The interaction between drivers through congestion effects constitutes a nonatomic multiclass congestion [27] game $\mathbb{G}$ with nonlinear cost functions $\boldsymbol{c} = (c_{s,r})$ defined in (3). In such frameworks, the vehicle users reach a particular distribution of choices between the possible paths, called a Wardrop Equilibrium (WE), where no user has an interest to change her choice unilaterally:

Definition 1 (**Wardrop Equilibrium** [28]). *The global vehicle flow $\boldsymbol{x}^*$ is a Wardrop Equilibrium (WE) if and only if:*

$$\forall s \in \{g, e_0, e_1\}, \quad c_{s,r}(\boldsymbol{x}^*) \leq c_{s,r'}(\boldsymbol{x}^*), \tag{4}$$

for all paths r, r' with r such that $x^*_{s,r} > 0$.

The charging unit price λ_i at CSO's hub $i \in \mathcal{H}_{\mathrm{cso}}$ is a congestion cost determined by the CSO and is specified in the next section.

B. Charging Service Operator: sets charging price

A CSO adapts the charging unit prices at its hubs in order to maximize the difference between its revenues from EV charging and its electricity supplying costs. Here, it is supposed that there is only one CSO in the city to avoid a complex competition between several CSOs, which will be the focus of a future work. More precisely, this CSO does not own all the hubs of the city, otherwise it could set arbitrarily high prices and EVs of class e_0 would have no choice but to pay these prices. Instead, some hubs belong to the city for example with a constant charging unit price λ_S^0, supposed higher than λ_H^0, the one available at home. The set of all hubs is denoted $\mathcal{H}$ and the set of the CSO's hubs, $\mathcal{H}_{\mathrm{cso}}$.

At its hubs, the CSO determines the charging profile over working hours aggregated over all EVs such that their SoC is full at the end of the day. The charging unit price λ_i at each CSO's hub i can be lower than the one at city's hubs, λ_S^0. More precisely, λ_i depends on the total charging need of EVs at CSO's hub i and other electricity usages called nonflexible because of their nonshiftable operation. This nonflexible term corresponds for example to the consumption of a shopping mall attached to the hub. The CSO schedules EV charging in order to smooth the power load at its hubs and therefore reduce its electricity supplying costs (see next section for details). For each CSO's hub, the aggregated charging need is scheduled using a water-filling algorithm introduced in [29]. The CSO sets the charging unit prices λ_i based on the output of this algorithm.

The working hours are divided into T discrete time slots. Without loss of generality, these time slots have the same duration of a time unit. For each hub i, the CSO has to determine the energy $\ell_{i,t}$ which is charged during time slot t. Assuming that the charging power is constant during each time slot, $\ell_{i,t}$ also represents the constant power load of the charging operation at time slot t, as the duration of a time slot is a time unit. The total charging need L_i at hub i is equal to:

$$L_i(\boldsymbol{x_e}) = \sum_r \delta_{i_r,i} \sum_{j=0,1} x_{e_j,r_S} \ell_{e_j,r}, \tag{5}$$

with $\delta_{i_r,i} = 1$ or 0 whether or not the destination hub i_r associated to path r is hub i, and x_{e_j,r_S} the flow of EVs of

class e_j choosing path r and charging at hub i at the end of the path. Each hub i has its own nonflexible consumption of electricity $\ell_{i,t}^0$ at time slot t. Note that this nonflexible term can include local electricity production and be negative, but here it is supposed that $\ell_{i,t}^0 \geq 0$ to simplify notations. The water-filling algorithm minimizes a quadratic proxy [29] of the total load at hub i while making sure that all EVs leave the hub with full SoC:

$$G_i^* = \min_{(\ell_{i,t})} \sum_{t=1}^T \left(\ell_{i,t} + \ell_{i,t}^0\right)^2 \quad \text{s.t.} \sum_{t=1}^T \ell_{i,t} = L_i. \tag{6}$$

Note that the Vehicle to Grid (V2G) technology can be integrated into this model by allowing $\ell_{i,t}$ to be negative, while making sure that at each time slot the aggregated SoC remains inside tangible bounds[3]. However we chose not to consider V2G because in general injected electricity is not compensated financially yet and may be potentially harmful for the local distribution grid. Note also that battery health limitations (depth of discharge, number of cycles...) cannot be integrated as it is because only the aggregated charging loads at each hub are modeled. A way to consider it however should be to assign a different charging power limit to each EV class depending on its initial SoC. Assuming without loss of generality that $\left(\ell_{i,t}^0\right)_t$ is increasingly sorted, the water-filling solution of this problem depends on the aggregated charging need L_i:

$$G_i^*(L_i) = \frac{\left(L_i + L_{i,t_0}^0\right)^2}{t_0(L_i)} + \sum_{t=t_0+1}^T \left(\ell_{i,t}^0\right)^2, \tag{7}$$

where $L_{i,t}^0 = \sum_{s \leq t} \ell_{i,s}^0$ and $t_0(L_i) \geq 1$ is such that $L_i \in \,]\Delta_{t_0}; \Delta_{t_0+1}]$, with $\Delta_t = t \times \ell_{i,t}^0 - L_{i,t}^0$ for $t \leq T$ and $\Delta_{T+1} = +\infty$. The corresponding optimal aggregated charging profile is $\ell_{i,t}^* = 0$ for $t > t_0$, and for $t \leq t_0$:

$$\ell_{i,t}^*(L_i) = \frac{L_i + L_{i,t_0}^0}{t_0(L_i)} - \ell_{i,t}^0. \tag{8}$$

Then, the CSO sets the charging unit price λ_i at hub i as a function of G_i^*. In this work we use the Locational Marginal Pricing (or LMP), in which λ_i is the derivative of G_i^*, which is proven to be the most efficient way to incite users to reduce G_i^* [30]. Our model can be adapted to other pricing mechanisms, like the average CSO's cost [24]. More precisely, λ_i is set to be proportional to the LMP as follows:

$$\lambda_i(\alpha, L_i) = \alpha \times \frac{\mathrm{d}G_i^*}{\mathrm{d}L_i} = 2\alpha \frac{L_i + L_{i,t_0}^0}{t_0(L_i)}, \tag{9}$$

with α the variable with which the CSO optimizes its payoff. This variable is the same for all CSO's hubs i and can be seen as a conversion parameter from marginal energy costs $\mathrm{d}G_i^*/\mathrm{d}L_i$ (kW²/kWh) of all of its hubs i into reasonable monetary prices λ_i (€/kWh) in order to maximize its payoff. As λ_i is a function of L_i, the charging unit price at CSO's hub i is a congestion cost like travel duration, i.e. depends on the number of EVs charging at hub i. Note that the CSO does not

---

[3]Min/max capacity of the "aggregated battery" connected to a given hub, where the max. bound is the sum of capacities of individual EVs plugged-in.
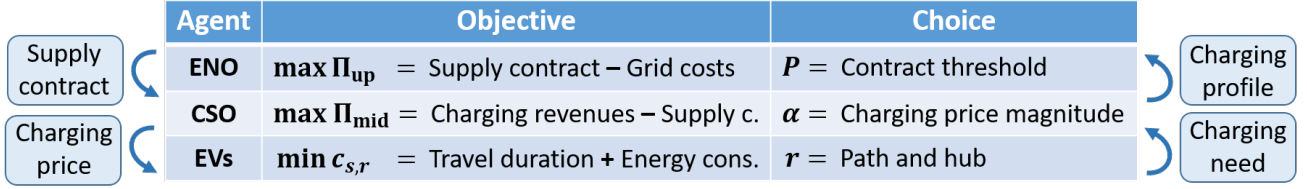
Agent	Objective		Choice	
ENO	$\max \Pi_{\mathrm{up}}$	$=$ Supply contract − Grid costs	$P =$	Contract threshold
CSO	$\max \Pi_{\mathrm{mid}}$	$=$ Charging revenues − Supply c.	$\alpha =$	Charging price magnitude
EVs	$\min c_{s,r}$	$=$ Travel duration + Energy cons.	$r =$	Path and hub

Fig. 2: Diagram of the different agents, their decision variables and their interactions.

change the structure of the charging unit prices at its hubs (as locational marginal prices), but only their order of magnitude.

As G_i^* is a nondecreasing function of L_i (see (7)), variable α must be nonnegative in order to have $\lambda_i \geq 0$. Moreover, it is assumed that some regulator sets an upper-bound $\overline{\alpha}$ to the CSO's decision variable. The feasible set of the CSO's strategy is denoted $\mathcal{A} = \{\alpha \in \mathbb{R} \mid 0 \leq \alpha \leq \overline{\alpha}\}$. The CSO wants to optimize its net payoff, the difference between its revenues and its costs. Its revenues are what EVs pay to be charged at CSO's hubs, and its costs come from the electricity supplying contracts with the ENO, which are described in next section.

C. Electrical Network Operator: designs CSO supply contract

In this urban framework, only the medium-voltage distribution grid and its operator the ENO are considered, and not the possible interactions with low-voltage distribution and the transmission grids. This ENO specifies the electricity supplying contract with the CSO to engage grid costs reductions. The CSO has to pay the ENO the supplying costs $C_{i,t}$ for the energy used to charge EVs at CSO's hub i and time slot t. The ENO determines one of the parameters of the contracts, a power threshold P, which is the same for all hubs and time slots. Whether the total load at given hub and time slot is above or below this threshold P, the CSO's electricity bill varies.

The total load at CSO's hub i and time slot t is made of the optimal aggregated charging profile given by the water-filling algorithm and the nonflexible part, and is equal to $\ell_{i,t}^{\mathrm{tot}} = \ell_{i,t}^* + \ell_{i,t}^0$. If the total load $\ell_{i,t}^{\mathrm{tot}}$ is below the power threshold P, the price per energy unit is $\mu(P)$, otherwise, the unit price of the exceeding load is $\overline{\mu}(P) > \mu(P)$. Functions μ and $\overline{\mu}$ are increasing: the higher the power threshold P prescribed to the CSO, the higher the price per energy unit. To simplify, linear functions are used: $\mu(P) = qP$ and $\overline{\mu}(P) = \overline{q}P$ with $\overline{q} > q$. The total supplying costs for both the charging and the nonflexible consumption at hub i and time slot t are given by the following function C, and the supplying costs $C_{i,t}$ only due to charging are defined on a pro rata basis:

$$C_{i,t}(L_i, P) = \frac{\ell_{i,t}^*(L_i)}{\ell_{i,t}^{\mathrm{tot}}(L_i)} \times C\left(\ell_{i,t}^{\mathrm{tot}}(L_i), P\right), \quad \text{where} \quad (10)$$

$$C\left(\ell_{i,t}^{\mathrm{tot}}, P\right) = \mu(P)\min\left(\ell_{i,t}^{\mathrm{tot}}, P\right) + \overline{\mu}(P)\max\left(0, \ell_{i,t}^{\mathrm{tot}} - P\right).$$

Note that even if threshold P is the same for all CSO's hubs, the supplying cost functions $C_{i,t}$ for EV charging are different due to the different nonflexible loads $\ell_{i,t}^0$ at each hub i.

For each time slot t, the ENO's cost $\mathcal{G}_t$ is defined as the marginal grid costs associated with EV charging. The grid costs are modeled as a quadratic proxy of the apparent power at the head of the city's grid. If S_t is the apparent power required to meet the total energy demand $\left(\ell_{i,t}^{\mathrm{tot}}\right)_i$ during time slot t, and S_t^0 the one corresponding to the nonflexible demand $\left(\ell_{i,t}^0\right)_i$ only, then the ENO's cost can be expressed as $\mathcal{G}_t = (S_t)^2 - (S_t^0)^2$. Note that at hubs $j \notin \mathcal{H}_{\mathrm{cso}}$ which do not belong to the CSO, EVs are supposed to plug and charge: $\ell_{j,1}^* = L_j$ and $\ell_{j,t}^* = 0$ if $t > 1$. The apparent power is obtained by solving the power flow equations from the Bus Injection Model [31], which correspond to the power balance at each bus (between the given power production/load $S_{0,k}$ at bus k and power flows S_k from/to the bus):

$$S_{0,k} = U_k \sum_{m \in X_k} \overline{Y_{k,m} U_m} \ (= S_k), \quad (11)$$

with U_k the complex voltage at bus k, X_k the set of buses connected to bus k and $Y_{k,m}$ the admittance of the line between buses k and m.

The ENO's objective can then be expressed as:

$$\Pi_{\mathrm{up}}(P, \boldsymbol{L}) = \sum_{t=1}^{T} \left(\sum_{i \in \mathcal{H}_{\mathrm{cso}}} C_{i,t}(L_i, P) - \beta \times \mathcal{G}_t(\boldsymbol{\ell}_t^*) \right), \quad (12)$$

with $\boldsymbol{L} = (L_i)_i$ and β a parameter which transforms $\mathcal{G}_t$ into a monetary cost. The ENO's decision variable, the power threshold $P \geq 0$, is supposed to be bounded by $\overline{P}$ by some regulator. The feasible set of the ENO's strategy is denoted $\mathcal{P} = \{P \in \mathbb{R} \mid 0 \leq P \leq \overline{P}\}$. Note that the ENO's objective depends on $\boldsymbol{L}$, the result of drivers' strategies, which depends itself on ENO's decision variable P, as shown in the next section. The different agents, their decision variables and their interactions are summarized in Fig. 2.

III. THE TRILEVEL OPTIMIZATION PROBLEM

Last section introduced the three types of agents in our smart charging framework and their interactions. This section focuses on the outcome of such a system. The following multilevel optimization problem is solved by the ENO as the decision maker at the upper level of the decision process. In particular, the ENO aims to maximize its objective function denoted Π_{up}. Note that the electricity supplying contract between the ENO and CSO, and the charging unit prices at CSO's hubs are long-term strategies (resp. of the ENO and CSO). They are assumed to be based on the forecast of drivers' behavior on a specific working day, forecast which is the Wardrop Equilibrium (WE) vehicles naturally reach and which depends on the charging unit prices (see next section). For example, the ENO might be pessimistic and optimizes

its net payoff on a worst-case-scenario day (e.g., with a high proportion of EVs on the roads).

The information available for each agent is as follows. The drivers know their costs functions on this specific working day: they observe the charging unit price functions chosen by the CSO. Therefore they can choose the optimal path and place to charge during this working day, corresponding to the WE of this day. The CSO has access to the behavior model of vehicle users and knows the main characteristics of the problem, such as the transportation network properties, the travel demands between origins O and destinations D, etc. Therefore, the CSO can compute the WE for any charging unit prices it chooses. However, the CSO has no information on the grid topology and consequently on ENO's costs, so that it does not know how the ENO chooses the supplying contract. Thus, the CSO must observe its supplying contract only once it is chosen by the ENO. Finally, the ENO has also access to the behavior model of vehicle users and to general information (e.g., travel demands), including the structure of the charging unit prices, which is assumed to be publicly disclosed by the CSO. This way, the ENO can compute the WE, the CSO's revenues and then CSO's reaction to its supplying costs (chosen by the ENO). This constitutes a trilevel optimization problem as illustrated on Fig. 2, with the ENO at the upper level, the CSO at the middle one and the drivers at the lower level.

A. Vehicle users at Wardrop Equilibrium

Before defining the trilevel optimization problem, some details about the lower level are needed. On the working day considered, the city's commuters have to choose how to get to their workplace and whether they charge their vehicle during the working hours. Due to the congestion effects on the road and also on the charging unit prices at CSO's hubs, the decision of a driver depends on the others'. The solution concept used to study this interaction is the Wardrop Equilibrium (see Definition 1). Such equilibria can be computed via Beckmann function [32]:

Proposition 1. *For any CSO's strategy α, the local minima of the following constrained optimization problem are WE of $\mathbb{G}$:*

$$\min_{\boldsymbol{x} \in X} \mathcal{B}(\boldsymbol{x}, \alpha), \quad with \tag{13}$$

$$\mathcal{B}(\boldsymbol{x}, \alpha) = \sum_a \int_0^{x_a} d_a + \sum_{(s,r) \in \mathcal{S}} x_{s,r} \left(t_{i_r} + \ell_{s,r} \lambda_{s,r} \right) + \alpha \sum_{i \in \mathcal{H}_{cso}} \mathcal{G}_i^*(\boldsymbol{x}_e)$$

$$X = \left\{ (x_{s,r})_{s,r} \mid x_{s,r} \geq 0, \ \sum_{r \in OD} x_{s,r} = X_s^{OD} \right\},$$

with $x_a = \sum_{\{r \ s.t. \ a \in r\}} \sum_s x_{s,r}$ the total vehicle flow on arc a, $\mathcal{S} = \{(e_j, r_S) \ s.t. \ i_r \notin \mathcal{H}_{cso}, \ (g,r), \ (e_1, r_H)\}$ and X_s^{OD} the portion of class s vehicles with origin O and destination D.

Unfortunately, for some CSO's strategies $\alpha \in \mathcal{A}$, there might be several minima of (13) and therefore, several WE. However, the following proposition shows (proof in Appendix B) that even if there are several WE, they all lead to the same congestion $d_a^*(\alpha)$ on each road a and the same

total charging need $L_i^*(\alpha)$ at CSO's hub i. Therefore, for given strategies α and P, the CSO and the ENO can expect a unique drivers' impact on their metrics, respectively on CSO's hubs and on the electrical grid.

Proposition 2. *Let the CSO's strategy be any $\alpha \in \mathcal{A}$. Any different WE $\boldsymbol{x}, \boldsymbol{y}$ of game $\mathbb{G}$ verify:*

$$\forall a, \ x_a = y_a, \qquad \forall i \in \mathcal{H}_{cso}, \ L_i(\boldsymbol{x}) = L_i(\boldsymbol{y}). \tag{14}$$

Note that total charging needs at WE depend on α, CSO's decision variable (see the expression of $\mathcal{B}(\boldsymbol{x}, \alpha)$ in (13)). According to Prop. 1 and 2, any solution of optimization problem (13) gives the unique $\boldsymbol{L}^*(\alpha) = (L_i^*(\alpha))_{i \in \mathcal{H}_{cso}}$ at WE.

B. The trilevel problem formulation

As mentioned in Sec. II-B, the objective Π_{mid} of the CSO is the difference between its charging revenues and its electricity supplying costs. At each CSO's hub i, the revenue R_i is the product between the charging unit price λ_i and the total charging need L_i at this hub. The CSO knows, for each $\alpha \geq 0$, that this need is the unique $L_i^*(\alpha)$ when drivers are at equilibrium, so that the revenue from hub i can be written:

$$R_i(\alpha, L_i^*(\alpha)) = L_i^*(\alpha) \times \lambda_i(\alpha, L_i^*(\alpha)). \tag{15}$$

In function of ENO's strategy P, the CSO has to minimize over $\alpha \in \mathcal{A}$ the following objective:

$$\Pi_{mid}(\alpha, P, \boldsymbol{L}^*(\alpha)) = \sum_{i \in \mathcal{H}_{cso}} \left(R_i(\alpha) - \sum_{t=1}^T C_{i,t}(L_i^*(\alpha), P) \right) \tag{16}$$

For each CSO's strategy $\alpha \in \mathcal{A}$, the ENO knows the global charging need $\boldsymbol{L}^*(\alpha)$ at WE. However, as the objective function Π_{mid} is not convex, Π_{mid} might have several global optima α^*.

In this work, it is supposed that there is a minimal cooperation between the CSO and the ENO, which leads to an optimistic formulation of the multilevel problem. This optimistic assumption states that for any ENO's strategy P, the global optimum α^* of (16) which gives the highest ENO's objective $\Pi_{up}(P, \boldsymbol{L}^*(\alpha^*))$ is chosen. Finally, the global trilevel optimization problem to solve is:

$$\max_{P \in \mathcal{P}, \alpha^* \in \mathcal{A}} \Pi_{up}\left(P, \boldsymbol{L}^*(\alpha^*)\right), \tag{17a}$$

$$\text{s.t.} \quad \Pi_{mid}(\alpha^*, P, \boldsymbol{L}^*(\alpha^*)) = \overline{\Pi_{mid}}(P), \tag{17b}$$

$$\text{s.t.} \quad \boldsymbol{L}^*(\alpha^*) = \boldsymbol{L}\left(\arg\min_{\boldsymbol{x} \in X} \mathcal{B}(\boldsymbol{x}, \alpha^*)\right), \tag{17c}$$

where $\overline{\Pi_{mid}}(P) = \max_{\alpha \in \mathcal{A}} \Pi_{mid}(\alpha, P, \boldsymbol{L}^*(\alpha))$ and function $\arg\min$ returns the set of global minima of $\mathcal{B}$, which share the same $\boldsymbol{L}^*$ (see Prop. 2).

This trilevel problem can be seen as a Stackelberg game (between the upper and middle levels) with equilibrium constraints (lower level) [33]. Note that depending on the information available to the ENO and CSO, other trilevel frameworks can be considered: if both the CSO and the ENO know the reactions of the other, they play in a simultaneous Nash game, with equilibrium constraints (lower level). However, solving this Nash game with algorithms such as Best Response may not converge due to the equilibrium constraints.

C. Iterative method based on literature review

In this section the most commonly used model of EV charging incentives in coupled electrical-transportation systems [12], [13] is introduced briefly. In this reference model, the EV lower level is the same as the one in the new trilevel model introduced in this paper. However, the different operators of the electrical system (CSO and ENO) are gathered into a unique System Operator (SO), which chooses the charging unit prices at its hubs which directly minimize the grid costs $\mathcal{G} = \beta \sum_t \mathcal{G}_t$ (instead of maximizing CSO's payoff). To this end, the SO uses the following LMP function in order to determine the charging price for each hub i:

$$\lambda_i(\boldsymbol{L}) = \tilde{\alpha} \times \frac{\mathrm{d}\mathcal{G}(\boldsymbol{\ell})}{\mathrm{d}L_i}, \tag{18}$$

which is the derivative of grid costs $\mathcal{G}$ obtained with power flow computations (11) instead of the local quadratic proxy (6). Parameter $\tilde{\alpha}$ converts marginal grid costs into reasonable charging prices like CSO's decision variable α. However, no method to fix $\tilde{\alpha}$ is available in the literature.

Note that papers using this method have no smart charging algorithm, so here the whole EV battery need is assumed to be charged during the first time slot: $\ell_1 = \boldsymbol{L}$ (method referred to as LMP+P&C in numerical Sec. V, for Plug and Charge). However, it is possible to consider an improved method (referred to as LMP+SC, for "Smart Charging") by solving the following charging scheduling problem:

$$\mathcal{G}^* = \min_{(\ell_{i,t})} \sum_{t=1}^{T} \beta \mathcal{G}_t(\boldsymbol{\ell}_t) \quad \text{s.t. } \forall i, \ \sum_{t=1}^{T} \ell_{i,t} = L_i. \tag{19}$$

Both alternative methods (LMP+P&C and LMP+SC) follow an iterative process: they alternatively compute the aggregated charging needs $\boldsymbol{L}^{(0)}$ at WE corresponding to charging unit prices $\boldsymbol{\lambda}^{(0)}$, then compute $\boldsymbol{\lambda}^{(1)}$ using (18) then update the charging needs $\boldsymbol{L}^{(1)}$ and so on. Note that there is no proof of convergence of this iterative process in the literature.

IV. RESOLUTION OF TRILEVEL OPTIMIZATION PROBLEM

A. An iterative method for upper and middle levels optimization

In most multilevel optimization problems, the convex lower level is replaced by the corresponding Karush-Kuhn-Tucker (KKT) conditions [34], which would transform the trilevel problem (17) into a bilevel (upper-middle) one with equilibrium constraints. However, using KKT conditions introduces integer variables and therefore transforms the global optimization problem into a mixed-integer nonlinear optimization problem, which increases dramatically the computational complexity [35]. In our setting we found that it was much faster to rather keep the initial trilevel structure (17) and simply solve the convex lower level using sequential least squares programming [36]. Thus, for the resolution of the global problem, we focus on the upper (ENO) and middle (CSO) levels. The lower level is referred to as an implicit numerical function $\boldsymbol{L}^*(\alpha)$ of CSO's price strategy α (see Prop. 2), which is the global charging need when vehicle users

---

Algorithm 1: Iterative global algorithm

Input: $P_0, \alpha_0, k = 0$
1 **Notation:** $\Pi_{\mathrm{mid}}(\alpha, P) \leftarrow \Pi_{\mathrm{mid}}(\alpha, P, \boldsymbol{L}^*(\alpha))$
2 $\overline{\alpha}_0 = \arg\max_\alpha \Pi_{\mathrm{mid}}(\alpha, P_0)$
3 **while** $\Pi_{mid}(\alpha_k, P_k) < \Pi_{mid}(\overline{\alpha}_k, P_k) - \varepsilon_{mid}$ **do**
4 $\quad k \leftarrow k + 1$
5 $\quad$ (i) $(P_k, \alpha_k) = \arg\max_{P,\alpha} \Pi_{\mathrm{up}}(P, \boldsymbol{L}^*(\alpha))$ $\quad$ (21)
6 $\qquad$ s.t. $\forall l < k, \Pi_{\mathrm{mid}}(\alpha, P) \geq \Pi_{\mathrm{mid}}(\overline{\alpha}_l, P) - \varepsilon_{mid}/3$
7 $\qquad$ solved with simulated annealing (**Algorithm 2**)
8 $\quad$ (ii) $\overline{\alpha}_k = \arg\max_\alpha \Pi_{\mathrm{mid}}(\alpha, P_k)$ $\quad$ (22)
9 $\qquad$ solved with Brent's method [38]

Output: P_k, α_k

Algorithm 2: Simulated annealing solving (21)

Input: $N_r, (\overline{\alpha}_l)_l, \eta, k = 0$
1 **while** $k < N_r$ **do**
2 $\quad k \leftarrow k + 1$
3 $\quad P$ uniformly chosen, $\alpha_P = \arg\max_{\overline{\alpha}_l} \Pi_{\mathrm{mid}}(\overline{\alpha}_l, P)$
4 $\quad$ **while** (P, α) *not feasible* **do**
5 $\qquad \alpha$ randomly chosen from $\mathcal{N}(\alpha_P, \eta)$
6 $\quad$ **Acceptance:** $k = 0$, with probability $\gamma_{\boldsymbol{z},n}(P, \alpha)$

Output: Accepted (P, α) giving maximal Π_{up}

---

are at equilibrium. The global trilevel optimization problem is rewritten as:

$$\max_{P \in \mathcal{P}, \alpha^* \in \mathcal{A}} \Pi_{\mathrm{up}}(P, \boldsymbol{L}^*(\alpha^*)),$$
$$\text{s.t. } \Pi_{\mathrm{mid}}(\alpha^*, P, \boldsymbol{L}^*(\alpha^*)) \geq \overline{\Pi_{\mathrm{mid}}}(P) - \varepsilon_{\mathrm{mid}}, \tag{20}$$

with $\varepsilon_{\mathrm{mid}} > 0$ a tolerance level introduced to guarantee the convergence of the algorithm suggested to solve (20). Note that a pessimistic version of Algorithm 1 introduced below can be used instead of the optimistic formulation (20). To ease notations, $\Pi_{\mathrm{mid}}(\alpha^*, P, \boldsymbol{L}^*(\alpha^*))$ is written $\Pi_{\mathrm{mid}}(\alpha^*, P)$, but note that both the computation of Π_{mid} and Π_{up} requires $\boldsymbol{L}^*$, i.e. to solve the convex lower level optimization.

The global trilevel problem (20) is solved using Algorithm 1, which is a simplified version of the iterative bounding algorithm introduced in [37], as there are no constraints at the upper and middle levels other than variable bounds. In Algorithm 1, the global optimization problems (21) and (22) at each iteration are solved by algorithms detailed in next section, but any other suitable algorithms can be applied. By definition of $\overline{\alpha}_k$, if the solution of (21) at an iteration of Algorithm 1 verifies the stopping criteria, then it is a solution of the initial trilevel problem (20). The convergence of Algorithm 1 is guaranteed by the following proposition (proved in Appendix C).

Proposition 3. *Algorithm 1 stops after a finite number of steps K and delivers an output (P_K, α_K) solution of* (20).

B. CSO and ENO optimization problems: a simulated annealing approach

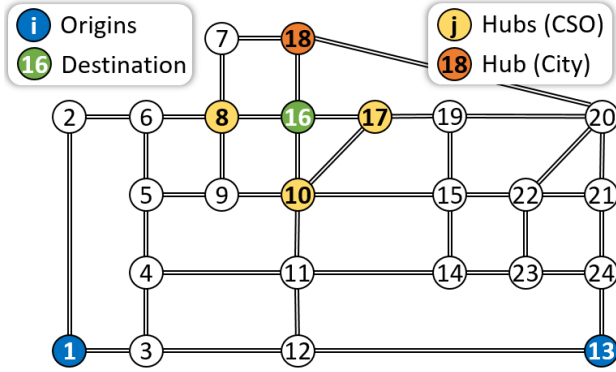Solving the optimization problems (21) and (22) of Algorithm 1 requires a global optimization method for nonconvex

Fig. 3: Sioux falls transportation network. *Commuters come from two different origins and have the same destination. They choose at which hub to park and the path to get there.*

Fig. 4: IEEE 33-bus medium-voltage distribution network.

and nondifferentiable objectives with continuous constraints. A natural candidate [39] is the simulated annealing method introduced in [40]. The principle is to explore a sufficient number of random feasible couples (P, α). The stopping criterion chosen is based on the concept of acceptance, where a potential couple (P, α) is accepted with probability:

$$\gamma_{\boldsymbol{z},n}(P,\alpha) = \min\left(1, \exp\left(\frac{\Pi_{\mathrm{up}}(P, \boldsymbol{L}^*(\alpha)) - \Pi_{\mathrm{up}}(\boldsymbol{z})}{|\Pi_{\mathrm{up}}(\boldsymbol{z})| \times K(n)}\right)\right) \quad (23)$$

with $\boldsymbol{z}$ the last accepted couple and K a function of the number of iterations n, here chosen as $K(n) = 0.99^n$. Note that a couple giving a lower Π_{up} than the last accepted couple may be accepted, although it becomes less likely after many iterations (decreasing K). Following [41], the algorithm stops when no couple (P, α) has been accepted N_r iterations in a row.

Note that solving scalar optimization (22) is much faster using scalar algorithms like Brent's method [38] rather than simulated annealing. For problem (21), the difficulty with simulated annealing is to randomly find feasible couples (P, α), i.e. which verify the constraints in (21): $\forall l < k$, $\Pi_{\mathrm{mid}}(\alpha, P,) \geq \Pi_{\mathrm{mid}}(\overline{\alpha}_l, P) - \frac{\varepsilon_{\mathrm{mid}}}{3}$. However we observed that the optimum $\overline{\alpha}$ of $\Pi_{\mathrm{mid}}(\cdot, P)$ depends faintly on P because the variations of the electricity supplying costs $C_{i,t}(L_i^*(\alpha), P)$ due to P are small. Then for every $P \in \mathcal{P}$, the $\alpha \in \mathcal{A}$ such that (P, α) is feasible are in the neighborhood of $\overline{\alpha}_P$, with $\overline{\alpha}_P = \arg\max_{\overline{\alpha}_l} \Pi_{\mathrm{mid}}(\overline{\alpha}_l, P)$. Consequently, we suggest that $P \in \mathcal{P}$ should be uniformly chosen first and then α, drawn from a normal distribution $\mathcal{N}(\overline{\alpha}_P, \eta)$ with mean $\overline{\alpha}_P$ and standard deviation some parameter η to choose. The resulting simulated annealing method is described in Algorithm 2.

Our global multilevel problem is solved with Algorithm 1, which uses at each iteration global optimization Algorithm 2. This numerical resolution is applied in next section to illustrate how our model can help ENO and CSO make decisions. œ

V. CASE STUDIES

In this section, Algorithm 1 introduced in previous section is applied to our trilevel model to find the optimal strategies for the ENO and the CSO in function of exogenous parameters. The parameters of the problem are set as follows, unless otherwise specified: 1500 commuters drive from each origin
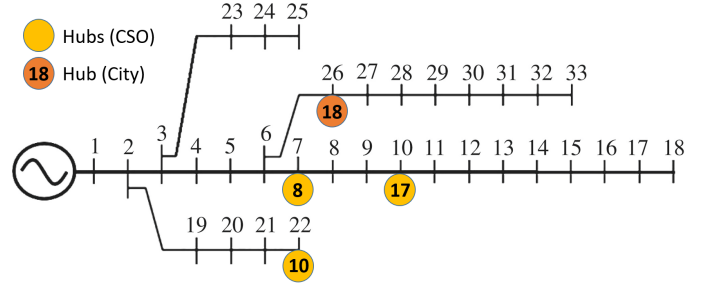
1 and 13 (3000 vehicles in total) of Sioux falls transportation network represented in Fig. 3, to destination 16. More precisely the drivers have to choose at which of the four hubs (at locations 8, 10, 17 and 18, the latter being owned by the city) they want to park and maybe charge. In Sec. V-A, hubs are supposed equally distant from destination and $t_i = 0$ without loss of generality. The constant charging unit price at city's hub is $\lambda_S^0 = 25$ c€/kWh, higher than the one at home, $\lambda_H^0 = 20$ c€/kWh. Half of vehicles are electric (except in Sec. V-A), and the two EV classes e_0 and e_1 are equally represented, with $s_0 = 5$ kWh and $s_1 = 0$ kWh. The length of the road between locations 3 and 4 is 2.5 km and the other lengths can be geometrically deduced from it. For all roads a, the speed limit is $v_a = 50$ km/h and the road capacity is $C_a = 0.2$ (i.e., travel duration triples if 20 % of the 3,000 vehicles take road a). The values of $\tau = 10$ €/h, $m_e = 0.2$ kWh/km, $m_g = 0.06$ L/km and $\lambda_g = 1.50$ €/L are taken from [24]. The four hubs belong to the IEEE 33-bus system illustrated in Fig. 4 and whose parameters are given in [42]. In particular, the total nonflexible consumption during working hours near each hub is respectively 1.51, 0.68, 0.45 and 0.45 MWh. Each hub's total nonflexible consumption is divided into a random profile over $T = 8$ time slots. The upper bounds for the ENO and the CSO's variables are set high enough to contain the optimal values: $\overline{\alpha} = 10^{-3}$ €/kW² and $\overline{P} = 4$ MW. The converting parameters are set as follows: $q = 0.1$ €/kW², $\overline{q} = 3q$ and $\beta = 10^{-3}$ €/kVA². Finally, the simulated annealing parameters $N_r = 15$ and $\eta = 2.5 \times 10^{-6}$ €/kW² have been adjusted with the help of brute-force search, to ensure a sufficient exploration of Π_{up} domain[4].

Before studying the global trilevel model in the next sections, the aggregated charging profiles (8) corresponding to the unique charging need L_i^* at equilibrium at each hub i (see Prop. 2) are illustrated in Fig. 5. This figure shows the local water-filling structure of these profiles (referred to as *Trilevel*) for each CSO's hub. Figure 5 also displays the charging profiles obtained solving (19), as in the LMP+SC method. Note that this profile is exclusively concentrated on the third time slot due to a lower nonflexible consumption than during the other time slots. For comparison, the P&C profile corresponding to $\boldsymbol{L}^*$ is also shown. It typically leads to significantly larger peak powers compared to the proposed water-filling scheduling and, in turn, higher grid costs.

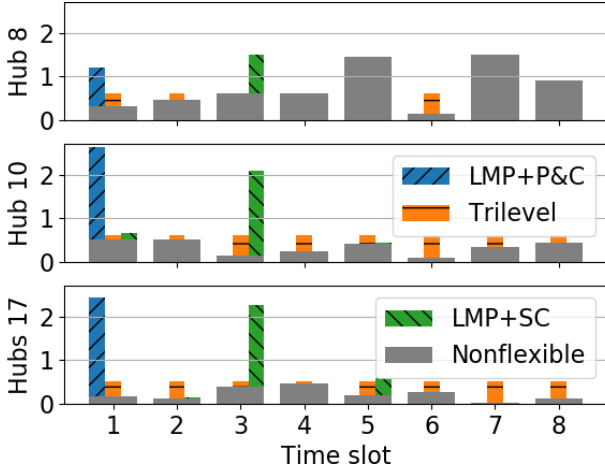[4]For example, above $N_r = 15$, the ratio accepted/explored points is no longer acceptable.

Fig. 5: Aggregated charging profiles for each CSO's hub, for the water-filling method (6) (*Trilevel*), the improved reference method (19) (LMP+SC) and the LMP+P&C method.

Fig. 6: Optimal ENO and CSO's payoffs (resp. Π_{up} and Π_{mid}) and normalized strategies (resp. $P^*/\overline{P}$ and $\alpha^*/\overline{\alpha}$) depending on EV penetration X_e. *When EV penetration goes over 75 %, CSO's payoff increases to the detriment of the ENO's because the ENO reduces the CSO's supplying contract.*

A. Sensitivity to Electric Vehicles penetration

Using our trilevel model, operators can find their optimal strategies as the proportion X_e of EVs among vehicles grows. More precisely, for each X_e value, Algorithm 1 gives the corresponding optimal payoffs and strategies for the ENO and the CSO (see Fig. 6). This figure shows that in general, both payoffs increase with X_e, as a higher X_e means more EV charging. Furthermore, in order to keep affordable charging prices at its hubs, the CSO has to reduce α as X_e increases and amplifies the price incentive part $\mathrm{d}G_i^*/\mathrm{d}L_i$ (see (9)). Note that when the number of EVs is high ($X_e \geq 85$ %), the ENO must lower the CSO's contract threshold P^*, otherwise the CSO would increase the monetary value α of smart charging to reduce its expensive supplying costs by inciting EVs to rather charge at city's hub. Thus, the ENO reduces its revenues from CSO's contract so that its payoff stagnates and CSO's payoff considerably increases.

For each EV penetration X_e, there is a unique charging need at each hub corresponding to vehicles' reaction to optimal strategies of the ENO and the CSO. Note that the uniqueness of the charging need at city's hub is not guaranteed by Prop. 2, but is invalidated only in specific cases (e.g., several city's hubs, specific ratios for roads' lengths and energy prices...). As these charging needs greatly increase with X_e, they are normalized by the total charging need aggregated over all hubs to emphasize their relative variations: $\tilde{L}_i = L_i / \sum_j L_j$ (see Fig 7). Note that different temporal profiles of the same nonflexible consumption (at each hub) lead to similar Fig. 6, but different normalized charging needs $\tilde{L}_i$. Figure 7 shows the $\tilde{L}_i$ for two different nonflexible consumption profiles. This figure reveals that the choice of hub by EVs depends greatly on the nonflexible consumption when the number of EVs is small, but less so as X_e increases. As the EV penetration increases, GVs are replaced by EVs, which enables more EVs to use closer hubs to the origins (as 10 and 17), to the detriment of city's hub 18. Note that fewer EVs choose hub 8 rather than hubs 10 and 17 due to the higher nonflexible consumption there (resp. 1.51 compared to 0.68 and 0.45 MWh).
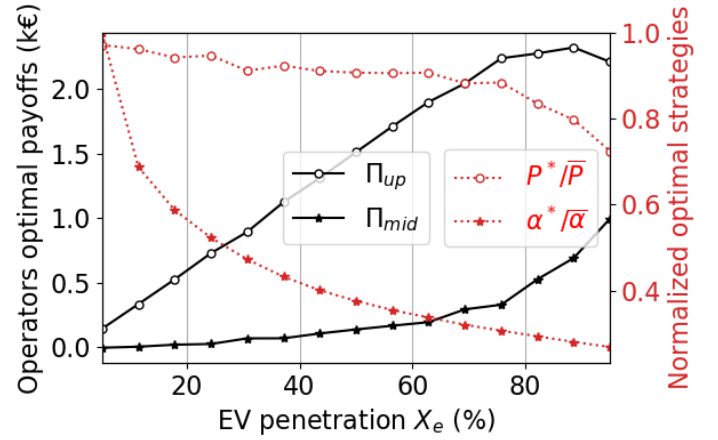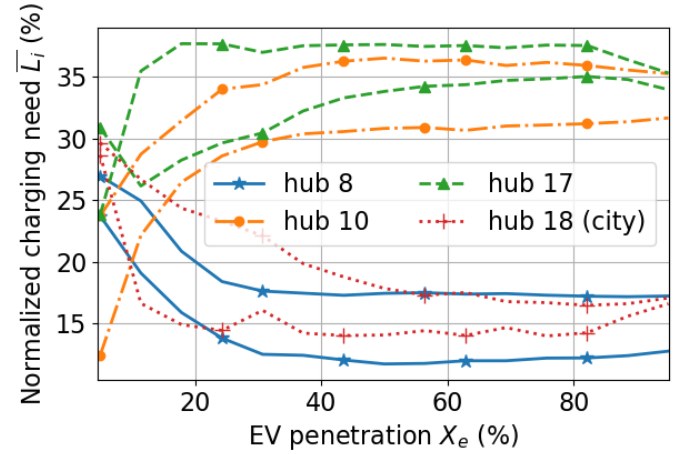

Fig. 7: Normalized charging needs $\tilde{L}_i = L_i / \sum_j L_j$ at all hubs depending on EV penetration X_e, for two different nonflexible consumption profiles. *The profile considered has a significant impact for low EV penetrations. For both profiles, $\tilde{L}_8$ and $\tilde{L}_{18}$ decrease with X_e because hub 18 is further away from the origins and hub 8 has a higher nonflexible consumption.*

B. Sensitivity to Public Transport fare

Last section was dedicated to the long-term EV penetration. This section focuses on the reaction of the ENO and CSO to an incentive coming from the transportation system. Here, it is supposed that city's hub 18 benefits from a subsidized Public Transport (PT) fare $t_{18} = 1$ €. We consider the PT fare t chosen by a transportation operator and that commuters pay to go from CSO's hubs to the destination: $t = t_8 = t_{10} = t_{17}$. Figure 8 shows the evolution of charging needs L_i at all hubs i in function of this PT fare. Note that all EVs of class e_1 charge at home: the CSO is better off with high enough charging prices even if it means fewer EVs charging at its hubs. For PT fares lower than $t = 2$ €, the number of EVs (of class e_0) choosing city's hub increases with t. Between $t = 2$ € and 3 €, this number drops because the PT fare
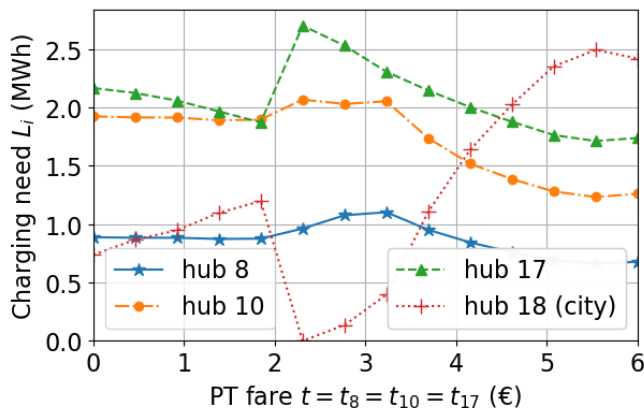
Fig. 8: Charging needs L_i at all hubs depending on the unique PT fare t. L_{18} *globally increases with t, except around $t = 2$ € where EVs charging at home choose to park at hub 18.*
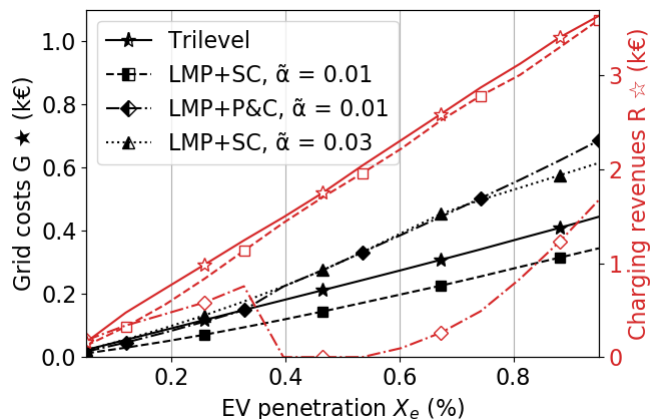

Fig. 9: ENO grid costs (solid lines) and CSO charging revenues (dashed lines), depending on EV penetration, obtained with our Trilevel method (star marker), the LMP+P&C one (diamond) and LMP+SC method for different normalizations $\tilde{\alpha}$ of the LMP (square and triangle). *The literature-based method may lead to minimal grid costs only if smart charging is considered and if $\tilde{\alpha}$ is carefully chosen (square marker). Charging revenues are always higher with Trilevel method.*

became too expensive for EVs charging at home, which instead all choose paths leading to city's hub 18. Then however, more and more EVs of class e_0 naturally choose the city's hub.

C. Comparison with iterative method based on literature

This section compares the trilevel model built in this paper with the most commonly used model of EV charging incentives in coupled electrical-transportation systems [12], [13] (see Sec. III-C), on the EV penetration sensitivity example of Sec. V-A. Figure 9 shows for each EV penetration X_e the grid costs $\mathcal{G}$ (filled black markers) and the charging revenues $\mathcal{R} = \sum_{i \in \mathcal{H}_{cso}} R_i$ (empty red markers) for the trilevel method (star marker), the improved iterative method (LMP+SC) for two values of $\tilde{\alpha}$, and the LMP+P&C method for $\tilde{\alpha} = 0.01$.

Figure 9 shows that for the same $\tilde{\alpha} = 0.01$ value, the LMP+P&C method (diamond marker) gives higher grid costs than the LMP+SC one (square), as expected, but also lower charging revenues: as grid costs are higher, the charging unit prices too so that EVs prefer to charge at city's hub (up to $X_e = 60$ %, where they accept these high prices because of the congested paths to access city's hub). The impact of the conversion parameter $\tilde{\alpha}$ is also illustrated in Fig. 9. For example, when $\tilde{\alpha}$ is too high (e.g., $\tilde{\alpha} = 0.03$), the LMP+SC method (triangle marker) gets similar results as the LMP+P&C one (diamond). Note that charging revenues are always higher in the trilevel model of this paper than in the other methods. This seems intuitive given that this metric is explicitly taken into account in the framework of this paper while the alternative methods focus on grid cost minimization.

Figure 9 illustrates that the trilevel model of this paper (star marker) obtains fairly low grid costs compared to the LMP+P&C method or the LMP+SC one with $\tilde{\alpha}$ not carefully designed. This indicates that the supplying contract, the proxy used in the scheduling problem (6) and the corresponding LMP (9) are good heuristics to reduce grid costs, as expressed in our previous paper [43]. Note that with a particular value $\tilde{\alpha} = 0.01$, the LMP+SC method (square marker) obtains the

minimal grid costs. This is made possible because the goal of the operator choosing the charging profiles and prices in this method is to precisely minimize grid costs. However in practice, the hubs' operator wants to maximize its payoff and may have no information on the electrical grid, as in the trilevel model of the present paper, which guarantees the highest charging revenues among all methods. Moreover, the results of the LMP+SC method are highly sensitive to the choice of parameter $\tilde{\alpha}$, as shown in Fig. 9. Finally, note that parallel computations are not practical for the iterative methods. Due to the complexity of solving scheduling problem (19), the LMP+SC method is actually slower (two times in average) to solve than the trilevel model, which has more optimization layers.

VI. CONCLUSION

In this work, the impact on the electrical system of EV commuting is modeled by a trilevel optimization problem. The lower, middle and upper levels respectively represent the EVs, interacting in a coupled driving-and-charging congestion game, the CSO which can modify the smart charging prices at its hubs and the ENO which revises the electricity supplying contracts with each hub. This trilevel problem is seen as a Stackelberg game (between the upper and middle levels) with equilibrium constraints (lower level), which is solved with an optimistic iterative algorithm combined with simulated annealing. For each ENO and CSO's strategies, we proved that there is a unique charging need at each hub when vehicles are at equilibrium. The behaviors' coupling between the three levels is illustrated on realistic urban networks, in function of the EV penetration and a transportation incentive. A comparison with a reference model in the coupled electrical-transportation literature shows the efficiency of the incentives (charging price and supplying contract) in our realistic trilevel model.

In a future work, several CSOs will interact in a game structure, making the trilevel problem an optimization at the upper level, combined with two games both at the middle and the lower levels. In parallel, a transportation operator (e.g., a public authority responsible for local pollution or dynamic road pricing) will be added to enable a theoretical study of the transportation-electrical coupling.

APPENDIX A
PROOF OF PROP. 1: WE COMPUTATION

Proof. A local minimum of (13) verifies the associated Karush–Kuhn–Tucker conditions. As λ_i is proportional to the derivative of G_i^* (see (9)), these conditions are equivalent to the Definition 1 of a WE. See [24] for more details. $\square$

APPENDIX B
PROOF OF PROP. 2: UNIQUE CHARGING NEEDS

Proposition 2 is due to the nondecreasing property of congestion and consumption costs. The proof of Prop. 2 requires the following lemma and definition.

Lemma 1. *For all CSO's strategies $\alpha \in \mathcal{A}$, the LMP function $\lambda_i^\alpha : L_i \mapsto \lambda_i(\alpha, L_i)$ defined in equation (9) is increasing.*

Proof. LMP function $\lambda_i^\alpha : L_i \mapsto 2\alpha \frac{L_i + L_{i,t_0}^0}{t_0(L_i)}$ is piecewise differentiable for all $\alpha \in \mathcal{A}$, with derivative $2\alpha/t_0(L_i) > 0$. We can conclude that λ_i^α is increasing by showing that it is continuous: if $L_i^+ = \Delta_t^+$ then $t_0(L_i^+) = t$ and $L_i^+ + L_{i,t}^0 = t\ell_{i,t}^0$ by definition of Δ_t. Similarly, if $L_i^- = \Delta_t^-$, then $t_0(L_i^-) = t-1$ and $L_i^- + L_{i,t-1}^0 = t\ell_{i,t}^0 - L_{i,t}^0 + L_{i,t-1}^0 = (t-1)\ell_{i,t}^0$ by definition of $L_{i,t}^0$. Therefore, $\lambda_i^\alpha(L_i^+) = \lambda_i^\alpha(L_i^-) = \ell_{i,t}^0$. $\square$

Definition 2 (Variational Inequality). *Let $Y \subseteq \mathbb{R}^N$ be a nonempty, closed and convex set. A vector $\boldsymbol{x} \in Y$ is a solution of the Variational Inequality VI($\boldsymbol{c}$, Y) if, for any vector $\boldsymbol{y} \in Y$:*

$$\boldsymbol{c}(\boldsymbol{x})^T (\boldsymbol{y} - \boldsymbol{x}) \geq 0. \tag{24}$$

Proof of Prop. 2. Let $\boldsymbol{x}, \boldsymbol{y} \in X$ be two WE of game $\mathbb{G}$. As functions d_a and λ_i (Lemma 1) are increasing, we have:

$$[\boldsymbol{c}(\boldsymbol{x}) - \boldsymbol{c}(\boldsymbol{y})]^T (\boldsymbol{x} - \boldsymbol{y}) = \sum_a (x_a - y_a)(d_a(x_a) - d_a(y_a))$$

$$+ \sum_{i \in \mathcal{H}_{cso}} \Big(L_i(\boldsymbol{x}) - L_i(\boldsymbol{y})\Big)\Big(\lambda_i^\alpha\big(L_i(\boldsymbol{x})\big) - \lambda_i^\alpha\big(L_i(\boldsymbol{y})\big)\Big) \geq 0,$$

which is equal to 0 if and only if (14) holds.

According to [44], WE $\boldsymbol{x}$ and $\boldsymbol{y}$ are solutions of $VI(\boldsymbol{c}, X)$. Equation (24) applied to $(\boldsymbol{x}, \boldsymbol{y})$ and $(\boldsymbol{y}, \boldsymbol{x})$ results in:

$$\big(\boldsymbol{c}(\boldsymbol{x}) - \boldsymbol{c}(\boldsymbol{y})\big)^T (\boldsymbol{x} - \boldsymbol{y}) \leq 0.$$

$\square$

APPENDIX C
PROOF OF PROP. 3: CONVERGENCE OF ALGORITHM 1

Proof. According to the maximum theorem (Beckmann function $\mathcal{B}$ continuous), the mapping $\boldsymbol{x}^*(\alpha)$ solution of (13) is upper hemicontinuous. As for a given α, all $\boldsymbol{x}^*(\alpha)$ lead to the same $\boldsymbol{L}^*(\alpha)$, function $L^*(\alpha)$ and therefore Π_{mid} are continuous. The same theorem states that $\overline{\Pi_{\text{mid}}}(P)$ is continuous because Π_{mid} is. As functions Π_{mid} and $\overline{\Pi_{\text{mid}}}$ are continuous respectively on compacts $\mathcal{A} \times \mathcal{P}$ and $\mathcal{P}$, they are uniformly continuous according to Heine–Cantor theorem, which gives δ_ε and $\overline{\delta}_\varepsilon$ verifying respectively:

$$\forall (\alpha_0, P_0), (\alpha_1, P_1) \in \mathcal{A} \times \mathcal{P} \text{ s.t. } \|(\alpha_0, P_0) - (\alpha_1, P_1)\| \leq \delta_\varepsilon,$$

$$\Pi_{\text{mid}}(\alpha_1, P_1) \geq \Pi_{\text{mid}}(\alpha_0, P_0) - \frac{\varepsilon_{\text{mid}}}{3} \tag{25}$$

$$\forall P_0, P_1 \in \mathcal{P} \text{ s.t. } |P_0 - P_1| \leq \overline{\delta}_\varepsilon, \ \overline{\Pi_{\text{mid}}}(P_0) \geq \overline{\Pi_{\text{mid}}}(P_1) - \frac{\varepsilon_{\text{mid}}}{3}.$$

Let $\delta = \min(\delta_\varepsilon, \overline{\delta}_\varepsilon)$. As $\mathcal{P}$ is compact, the sequence (P_k) built at each iteration of Algorithm 1 by (21) admits a subsequence $(P_{u(n)})$ which converges to P_{lim}. Then, by definition:

$$\exists N_\delta \in \mathbb{N}^* \text{ s.t. } \forall n \geq N_\delta, \quad |P_{u(n)} - P_{\text{lim}}| \leq \frac{\delta}{2}.$$

Let $k = u(N_\delta), K = u(N_\delta + 1)$. Then $|P_k - P_K| \leq \delta$, so that combining (25) with $(\overline{\alpha}_k, P_k), (\overline{\alpha}_k, P_K)$ gives:

$$\Pi_{\text{mid}}(\overline{\alpha}_k, P_K) \geq \Pi_{\text{mid}}(\overline{\alpha}_k, P_k) - \frac{\varepsilon_{\text{mid}}}{3} \geq \overline{\Pi_{\text{mid}}}(P_K) - \frac{2}{3}\varepsilon_{\text{mid}},$$

with $\overline{\alpha}_k$ given by (22) at iteration k. Finally, as (P_K, α_K) verifies constraint $l = k$ of (21), we have:

$$\Pi_{\text{mid}}(\alpha_K, P_K) \geq \Pi_{\text{mid}}(\overline{\alpha}_k, P_K) - \frac{\varepsilon_{\text{mid}}}{3},$$

$$\text{thus} \quad \Pi_{\text{mid}}(\alpha_K, P_K) \geq \overline{\Pi_{\text{mid}}}(P_K) - \varepsilon_{\text{mid}},$$

which means that the stopping criteria is reached after iteration K, and Algorithm 1 ends with (P_K, α_K) solution of (20). $\square$

REFERENCES

[1] IEA, "Global ev outlook 2020," tech. rep., IEA, 2020.

[2] RTE, "Integration of electric vehicles into the power system in france," tech. rep., RTE, May 2020.

[3] W. Wei, W. Danman, W. Qiuwei, M. Shafie-Khah, and J. P. Catalao, "Interdependence between transportation system and power distribution system: A comprehensive review on models and applications," *Journal of Modern Power Systems and Clean Energy*, vol. 7.3, pp. 433–48, 2019.

[4] H. Zhang, Z. Hu, and Y. Song, "Power and transport nexus: Routing electric vehicles to promote renewable power integration," *IEEE Transactions on Smart Grid*, vol. 11, no. 4, pp. 3291–3301, 2020.

[5] M. Ammous, S. Belakaria, S. Sorour, and A. Abdel-Rahim, "Joint delay and cost optimization of in-route charging for on-demand electric vehicles," *IEEE Trans. on Intelligent Vehicles*, 5(1), p 149-64, 2019.

[6] T. Qian, C. Shao, X. Wang, and M. Shahidehpour, "Deep reinforcement learning for ev charging navigation by coordinating smart grid and intelligent transportation system," *IEEE Transactions on Smart Grid*, vol. 11, no. 2, pp. 1714–1723, 2019.

[7] B. Sohet, Y. Hayel, O. Beaude, and A. Jeandin, "Learning pure nash equilibrium in smart charging games," in *2020 59th IEEE Conference on Decision and Control (CDC)*, pp. 3549–3554, IEEE, 2020.

[8] W. Yao, J. Zhao, F. Wen, Z. Dong, Y. Xue, Y. Xu, and K. Meng, "A multi-objective collaborative planning strategy for integrated power distribution and electric vehicle charging systems," *IEEE Transactions on Power Systems*, vol. 29, no. 4, pp. 1811–1821, 2014.

[9] J. Tan and L. Wang, "Real-time charging navigation of electric vehicles to fast charging stations: A hierarchical game approach," *IEEE Trans. on Smart Grid*, vol. 8, no. 2, pp. 846–856, 2017.

[10] X. Li, Y. Xiang, L. Lyu, C. Ji, Q. Zhang, F. Teng, and Y. Liu, "Price incentive-based charging navigation strategy for electric vehicles," *IEEE Trans. on Industry Applications*, vol. 56, no. 5, pp. 5762–5774, 2020.

[11] T. Yang, Q. Guo, L. Xu, and H. Sun, "Dynamic pricing for integrated energy-traffic systems from a cyber-physical-human perspective," *Renewable and Sustainable Energy Reviews*, vol. 136, p. 110419, 2021.

[12] M. Alizadeh, H.-T. Wai, M. Chowdhury, A. Goldsmith, A. Scaglione, and T. Javidi, "Optimal pricing to manage electric vehicles in coupled power and transportation networks," *IEEE Trans. on Control of Network Systems*, vol. 4, no. 4, pp. 863–875, 2016.

[13] W. Wei, L. Wu, J. Wang, and S. Mei, "Network equilibrium of coupled transportation and power distribution systems," *IEEE Trans. on Smart Grid*, vol. 9, no. 6, pp. 6764–6779, 2017.

[14] X. Shi, Y. Xu, Q. Guo, H. Sun, and W. Gu, "A distributed ev navigation strategy considering the interaction between power system and traffic network," *IEEE Trans. on Smart Grid*, to be published.

[15] T. Qian, C. Shao, X. Li, X. Wang, and M. Shahidehpour, "Enhanced coordinated operations of electric power and transportation networks via ev charging services," *IEEE Trans. on Smart Grid*, vol. 11, no. 4, pp. 3019–3030, 2020.

[16] W. Yuan, J. Huang, and Y. J. A. Zhang, "Competitive charging station pricing for plug-in electric vehicles," *IEEE Transactions on Smart Grid*, vol. 8, no. 2, pp. 627–639, 2015.

[17] H. Wu, M. Shahidehpour, A. Alabdulwahab, and A. Abusorrah, "A game theoretic approach to risk-based optimal bidding strategies for electric vehicle aggregators in electricity markets with variable wind energy resources," *IEEE Trans. on Sustainable Energy*, 7(1), p374-85, 2015.

[18] S. I. Vagropoulos, D. K. Kyriazidis, and A. G. Bakirtzis, "Real-time charging management framework for electric vehicle aggregators in a market environment," *IEEE Trans. on Smart Grid*, 7(2), p948-57, 2015.

[19] N. Alguacil, A. Delgadillo, and J. M. Arroyo, "A trilevel programming approach for electric grid defense planning," *Computers & Operations Research*, vol. 41, pp. 282–290, 2014.

[20] S. Jin and S. M. Ryan, "A tri-level model of centralized transmission and decentralized generation expansion planning for an electricity market," *IEEE Trans. on Power Systems*, vol. 29, no. 1, pp. 132–41, 2013.

[21] D. Aussel, L. Brotcorne, S. Lepaul, and L. von Niederhäusern, "A trilevel model for best response in energy demand-side management," *European Journal of Operational Research*, vol. 281, no. 2, pp. 299–315, 2020.

[22] B. Shakerighadi, A. Anvari-Moghaddam, E. Ebrahimzadeh, F. Blaabjerg, and C. L. Bak, "A hierarchical game theoretical approach for energy management of electric vehicles and charging stations in smart grids," *Ieee Access*, vol. 6, pp. 67223–67234, 2018.

[23] M. Alizadeh, H.-T. Wai, A. Goldsmith, and A. Scaglione, "Retail and wholesale electricity pricing considering electric vehicle mobility," *IEEE Trans. on Control of Network Systems*, vol. 6, no. 1, pp. 249–260, 2018.

[24] B. Sohet, Y. Hayel, O. Beaude, and A. Jeandin, "Coupled charging-and-driving incentives design for electric vehicles in urban networks," *IEEE Trans. on Intelligent Transportation Systems*, to be published.

[25] B. of Public Roads, "Traffic assignment manual," tech. rep., U.S. Department of Commerce, Urban Planning Division;, 1964.

[26] M. Jeihani, S. Lawe, and J. Connolly, "Improving traffic assignment model using intersection delay function," tech. rep., 2006.

[27] N. Jiang and C. Xie, "Computing and analysing mixed equilibrium network flows with gasoline and electric vehicles," *Computer-aided civil and infrastructure engineering*, vol. 29, no. 8, pp. 626–641, 2014.

[28] J. Wardrop, "Some theoretical aspects of road traffic research," *Proc Inst Civ Eng Part II*, vol. 1, pp. 325–278, 1952.

[29] A.-H. Mohsenian-Rad, V. W. Wong, J. Jatskevich, R. Schober, and A. Leon-Garcia, "Autonomous demand-side management based on game-theoretic energy consumption scheduling for the future smart grid," *IEEE Trans. on Smart Grid*, vol. 1, no. 3, pp. 320–331, 2010.

[30] R. Li, Q. Wu, and S. S. Oren, "Distribution locational marginal pricing for optimal electric vehicle charging management," *IEEE Trans. on Power Systems*, vol. 29, no. 1, pp. 203–211, 2013.

[31] J. Zhu, *Optimization of power system operation*. J. Wiley & Sons, 2015.

[32] M. Beckmann, C. McGuire, and C. Winsten, *Studies in the economics of transportation*. Research memorandum, Published for the Cowles Commission for Research in Economics by Yale University Press, 1956.

[33] A. Ehrenmann, *Equilibrium problems with equilibrium constraints and their application to electricity markets*. PhD thesis, Citeseer, 2004.

[34] B. Colson, P. Marcotte, and G. Savard, "An overview of bilevel optimization," *Annals of operations research*, vol. 153,1, pp. 235–56, 2007.

[35] K. Papadimitriou, C. H.; Steiglitz, *Combinatorial optimization: algorithms and complexity*. Dover Publications, 1998.

[36] P. T. Boggs and J. W. Tolle, "Sequential quadratic programming," *Acta numerica*, vol. 4, no. 1, pp. 1–51, 1995.

[37] A. Mitsos, P. Lemonidis, and P. I. Barton, "Global solution of bilevel programs with a nonconvex inner program," *Journal of Global Optimization*, vol. 42, no. 4, pp. 475–513, 2008.

[38] K. Chandram, N. Subrahmanyam, and M. Sydulu, "Brent method for dynamic economic dispatch with transmission losses," in *IEEE/PES Transmission and Distrib. Conference and Exposition*, pp. 1–5, 2008.

[39] A. Dekkers and E. Aarts, "Global optimization and simulated annealing," *Mathematical programming*, vol. 50, no. 1-3, pp. 367–393, 1991.

[40] H. E. Romeijn and R. L. Smith, "Simulated annealing for constrained global optimization," *Journal of Global Optim.*, 5(2), p101-26, 1994.

[41] B. W. Wah and T. Wang, "Simulated annealing with asymptotic convergence for nonlinear constrained global optimization," in *International Conf. on Principles and Practice of Constraint Prog.*, p461-75, 1999.

[42] M. E. Baran and F. F. Wu, "Network reconfiguration in distribution systems for loss reduction and load balancing," *IEEE Power Engineering Review*, vol. 9, no. 4, pp. 101–102, 1989.

[43] B. Sohet, Y. Hayel, O. Beaude, and A. Jeandin, "Impact of strategic electric vehicles driving behavior on the grid," in *IEEE PES ISGT 2020 Europe*, Oct. 2020.

[44] M. J. Smith, "The existence, uniqueness and stability of traffic equilibria," *Transportation Research Part B: Methodo.*, 13(4), p295-304, 1979.

Benoit Sohet graduated from École Normale Supérieure de Cachan in 2018. He received the M.Sc. degree in climate physics at Université de Paris-Saclay in 2017 and the M.Sc. degree in applied mathematics at ENSTA ParisTech in 2018. He is currently pursuing a Ph.D. in applied mathematics at EDF R&D and at Avignon Université. His research is related to game theory and its applications to the electrical and transportation systems.

Yezekael Hayel (M'08, SM'17) received the M.Sc. degree in computer science and applied mathematics from the University of Rennes 1 in 2002, and the Ph.D. degree in computer science from the University of Rennes 1 and INRIA in 2005. He is an Assistant/Associate Professor with the University of Avignon, France, since 2006. He has held a tenure position (HDR) since 2013. He was a Visiting Professor with the NYU Polytechnic School of Engineering from 2014 to 2015. He was the Head of the Computer Science/Engineering Institute with the University of Avignon from 2016 to 2019. His research interests include the performance evaluation and optimization of complex network systems based on game theoretic and queuing models. He was involved at applications in communication/ transportation and social networks, such as wireless flexible networks, bio-inspired and self-organizing networks, and economic models of the Networks. He is associate editor of the GAMES journal.

Olivier Beaude received the M.Sc. degree in applied mathematics and economics from École polytechnique, Palaiseau, France, in 2010, the M.Sc. degree in optimization, game theory, and economic modeling from Université Paris VI, Paris, France, in 2011, and the Ph.D. degree from the Laboratory of Signals and Systems, CentraleSupélec, and the Research and Development Center, Renault, France, in 2015. He is currently a Research Engineer with EDF Research and Development, where his research interests include controlling the impact of EV charging on the grid, and the development of coordination mechanisms, and incentives for local electricity systems.

Alban Jeandin holds an Engineering degree from Télécom Paris and École Nationale des Ponts et Chaussées, with specialization in telecommunications, intelligent transportation systems and smart cities. He joined EDF R&D in 2011. From 2011 to 2016, he was involved in the French smart metering roll out program. He is currently leading EDF R&D's research project on vehicle-grid integration and smart charging. His research interests include Smart Metering, Smart Grids, and impact of EV charging on the grid, data exchange standards for Smart Charging and V2G, and Smart Cities.